

Structural Characterization of Sol–Gel Derived Oxycarbide Glasses. 2. Study of the Thermal Stability of the Silicon Oxycarbide Phase

Laurence Bois, Jocelyne Maquet, and Florence Babonneau*

Chimie de la Matière Condensée, Université Pierre et Marie Curie, CNRS, 4 place Jussieu, 75005 Paris, France

Djamila Bahloul

Laboratoire des Céramiques Nouvelles, Faculté des Sciences de Limoges, 123 avenue A. Thomas 87060 Limoges, France

Received December 20, 1994. Revised Manuscript Received February 24, 1995[®]

A gel resulting from cohydrolysis of dimethyldiethoxysilane and tetraethoxysilane has been converted through pyrolysis at 1000 °C into a silicon oxycarbide glass. A previous study has shown that this system can be described as a silicon oxycarbide matrix ($\text{SiC}_{0.14}\text{O}_{1.64}$) in which a free carbon phase (≈ 8 wt %) is dispersed. Its chemical evolution at high temperatures from 1000 to 1600 °C was investigated using various structural techniques: ^{29}Si solid state magic angle spinning nuclear magnetic resonance (^{29}Si MAS NMR), Raman spectroscopy and X-ray diffraction (XRD). In the 1000–1300 °C temperature range, redistribution reactions between Si–O and Si–C bonds occur, which lead to an enrichment in SiO_4 and SiC_4 units. Above 1400 °C, small silicon carbide crystallites are formed through carbothermal reaction between the free carbon and the silicon oxycarbide phase. However, even at 1500 °C, the samples remain mainly amorphous. The oxidation behavior of the glasses was also investigated using thermogravimetric analysis coupled with mass spectrometry: despite the presence of a free carbon phase, the samples exhibit a high oxidation resistance.

Introduction

It is already known that anionic substitution of oxygen by nitrogen in a silica network improve the mechanical properties of the resulting silicon oxynitride glasses.^{1–3} Introduction of tetravalent carbon in a silica network using classical synthetic procedures was less successful: melting of a silica-based glass in the presence of silicon carbide leads to the incorporation of only 0.5 wt % of carbon; however, the oxycarbide glasses showed an improvement in mechanical properties.^{4,5} The sol–gel process is an attractive synthetic approach to silicon oxycarbide glasses, as revealed by the numerous studies recently published in this field.^{6–20} Si–C bonds can be introduced very easily in silica gels, using

organically modified silicon alkoxides.²¹ The pyrolysis of such gels above 1000 °C and under inert atmosphere leads to residues, which can be described as an intimate mixture of silicon oxycarbide and free carbon phases. The silicon oxycarbide phase is built on $\text{SiC}_x\text{O}_{4-x}$ units as clearly shown by ^{29}Si magic angle spinning nuclear magnetic resonance (MAS-NMR).^{7,8,10,12–20} The chemical composition of this phase is strongly related to the nature of the gel precursor and more precisely to the O/Si ratio.^{16,22} The presence of a free carbon phase was evidenced indirectly from the comparison between elemental analysis and quantitative analysis of the ^{29}Si NMR data.¹³ Its amount in the pyrolysis residue depends on the structure of the gel precursor, the nature of the organic substituents and the pyrolysis conditions (temperature and duration).²²

[®] Abstract published in *Advance ACS Abstracts*, April 1, 1995.

- (1) Loehman, R. E. *J. Non-Cryst. Solids* **1983**, *56*, 123.
- (2) Coon, D. N.; Rapp, J. G.; Bradt, R. C.; Pantano, C. G. *J. Non-Cryst. Solids* **1983**, *56*, 161.
- (3) Loehman, R. E. *J. Non-Cryst. Solids* **1980**, *42*, 433.
- (4) Homeny, J.; Risbud, S. H. *Mater. Lett.* **1985**, *3*, 432.
- (5) Homeny, J.; Nebon, G. G.; Risbud, S. H. *J. Am. Ceram. Soc.* **1988**, *71*, 386.
- (6) Chi, F. K. *Ceram. Eng. Proc.* **1983**, *4*, 704.
- (7) Babonneau, F.; Thorne, K.; Mackenzie, J. D. *Chem. Mater.* **1989**, *1*, 554.
- (8) Zhang, H.; Pantano, C. G. *J. Am. Ceram. Soc.* **1990**, *73*, 958.
- (9) Kamiya, K.; Yoko, T.; Tanaka, K.; Takeuchi, M. *J. Non-Cryst. Solids* **1990**, *121*, 182.
- (10) Laine, R. M.; Rahn, J. A.; Youngdahl, K. A.; Babonneau, F.; Hoppe, M. L.; Zhang, Z. F.; Harrod, J. F. *Chem. Mater.* **1990**, *2*, 464.
- (11) Hurwitz, F. I.; Farmer, S. C.; Terepka, F. M.; Leonhardt, T. A. *J. Mater. Sci.* **1991**, *26*, 1247.
- (12) Renlund, G.; Prochazka, S.; Doremus, R. H. (a) *J. Mater. Res.* **1991**, *6*, 2723; (b) *J. Mater. Res.* **1991**, *6*, 2716.

- (13) Babonneau, F.; Bois, L.; Livage, J. *J. Non-Cryst. Solids* **1992**, *147*, 148, 280.

- (14) Burns, G. T.; Taylor, R. B.; Xu, Y.; Zangvil, A.; Zank, G. A. *Chem. Mater.* **1992**, *4*, 1313.
- (15) Belot, V.; Corriu, R.; Leclercq, D.; Mutin, P. H.; Vioux, A. *J. Non-Cryst. Solids* **1992**, *147*, 148, 52.
- (16) Belot, V.; Corriu, R.; Leclercq, D.; Mutin, P. H.; Vioux, A. *J. Non-Cryst. Solids* **1992**, *144*, 287.
- (17) Singh, A. K.; Pantano, C. G. *Mater. Res. Soc. Symp. Proc.* **1992**, *271*, 795.
- (18) Babonneau, F.; Soraru, G. D.; D'Andrea, G.; Dire, S.; Bois, L. *Mater. Res. Soc. Symp. Proc.* **1992**, *271*, 789.
- (19) Hurwitz, F. I.; Heimann, P.; Farmer, S. C.; Hembree, D. M., Jr. *J. Mater. Science* **1993**, *28*, 6622.
- (20) Babonneau, F.; Bois, L.; Yang, C.-Y.; Interrante, L. V. *Chem. Mater.* **1994**, *6*, 51.
- (21) Schmidt, H.; Scholze, H.; Kaiser, A. *J. Non-Cryst. Solids* **1982**, *48*, 65.
- (22) Soraru, G. D. *J. Sol-Gel Sci. Technol.*, in press.

These sol-gel derived silicon oxycarbide glasses have interesting potential applications in the field of ceramic fibers^{11,23} and ceramic composites.^{24,25} High elastic modulus and flexural strength have already been reported.²⁶ These applications are, however, strongly related to their thermochemical and thermomechanical stability, which have received little attention in the literature.²⁷ It is well-known that in these systems, carbothermal reduction occurs at high temperatures ($T \geq 1500^\circ\text{C}$), leading to the formation of crystalline silicon carbide. In fact, these polysiloxanes have also been studied as potential SiC precursors.^{14,28-32}

A previous study was focused on the conversion of a siloxane-silica polymer prepared by cohydrolyzing dimethyldiethoxysilane (DMDES) and tetraethoxysilane (TEOS) in a 1/1 ratio into a silicon oxycarbide glass.³³ The pyrolysis process was analyzed in detail using thermogravimetric analysis coupled with mass spectrometry (TG/MS), multinuclear magic angle spinning nuclear magnetic resonance (²⁹Si, ¹³C, and ¹H MAS-NMR), infrared spectroscopy (IR), and electron spin resonance (ESR). The residue obtained after pyrolysis at 1000 °C can be described as an amorphous silicon oxycarbide phase mixed with a free carbon phase.

The objective of the present paper was to follow the chemical evolution of this silicon oxycarbide glass at high temperatures, up to 1500 °C, in order to investigate its thermal stability and crystallization behavior under inert atmosphere. The firing process has been characterized using ²⁹Si MAS NMR, chemical analysis, X-ray diffraction (XRD), and Raman spectroscopy. The oxidation behavior was also investigated using thermogravimetric analysis coupled with mass spectrometry.

Experimental Section

The preparation of the polysiloxane polymer has already been described.³³ Gels were prepared by mixing TEOS (Fluka) and DMDES (Fluka) in a 1/1 ratio. Acidic water (HCl, pH = 2) was then added ($\text{H}_2\text{O}/\text{TEOS} = 6$) and the mixture was stirred. No alcohol was used as solvent. The sol was then poured into plastic tubes and air dried at room temperature. The solution gelled within about 2 days. Heat treatment under flowing argon was carried out in a tubular furnace at 10 °C/min. The dried gel was finely ground and placed in graphite crucible.

²⁹Si MAS NMR spectra were recorded on a Bruker MSL400 spectrometer with 7 mm rotors and spinning rates of 4 kHz.

(23) Renlund, G. M. French Patent 90 06453.

(24) Hurwitz, F. I.; Hyatt, L.; Gorecki, J.; D'Amore, L. *Ceram. Eng. Sci. Proc.* **1987**, *8*, 732.

(25) Zhang, H.; Pantano, C. G. In *Ultrastructure Processing of Advanced Materials*; Uhlmann, D. R., Ulrich, D. R., Eds.; John Wiley & Sons: New York, 1991; p 223.

(26) Soraru, G. D.; Sglavo, V. M.; Diré, S.; D'Andrea, G.; Babonneau, F. In *Third Euro-Ceramics*; Duran, P., Fernandez, J. F., Eds.; Faenza Editrice Iberica S. L., **1993**, *2*, 1157.

(27) Zhang, H.; Pantano, C. G. *Mater. Res. Soc. Symp. Proc.* **1992**, *271*, 783.

(28) White, D. A.; Oleff, S. M.; Boyer, R. D.; Budinger, P. A.; Fox, J. R. (a) *Adv. Ceram. Mater.* **1987**, *2*, 45; (b) *Adv. Ceram. Mater.* **1987**, *2*, 53.

(29) Fox, J. R.; White, D. A.; Oleff, S. M.; Boyer, R. D.; Budinger, P. A. *Mater. Res. Soc. Symp. Proc.* **1986**, *73*, 395.

(30) Chen, K. C.; Thorne, K. J.; Chemseddine, A.; Babonneau, F.; Mackenzie, J. D. *Mater. Res. Soc. Symp. Proc.* **1988**, *121*, 571.

(31) Sugahara, Y.; Takeda, Y.; Kuroda, K.; Kato, C. *J. Non Cryst. Solids* **1988**, *100*, 542.

(32) Wei, G. C.; Kennedy, C. R.; Harris, L. A. *Ceram. Bull.* **1984**, *63*, 1054.

(33) Bois, L.; Maquet, J.; Babonneau, F.; Mutin, H.; Bahloul, D.; *Chem. Mater.* **1994**, *6*, 796.

Short pulsewidths of 2 μs ($\theta = 30^\circ$) and relatively long recycle delays of 60 s were used to account for long relaxation times. About 1000 transients were recorded with 125 kHz spectral width and 4K data points. Exponential line broadening (50 Hz) was applied before Fourier transform. The spectra were simulated with the program WINFIT³⁴ to extract the percentages of the various $\text{SiC}_x\text{O}_{4-x}$ units ($0 \leq x \leq 4$). $\text{SiC}_x\text{O}_{4-x}$ represents a Si site with x Si-C bonds and $(4-x)$ Si-O bonds.

Raman spectra were recorded on a Jobin-Yvon U1000 spectrometer using a Ar laser (457.9 nm excitation). The laser power was set to 80 mW. The spectra were recorded between 700 and 1800 cm^{-1} , with 1 cm^{-1} increment and acquisition time of 2 s. A 90° excitation collection geometry was used. The powdered sample was placed in a rotating sample holder to prevent excessive heating of the sample.

ESR experiments were run at room temperature on a Varian E09 spectrometer with a microwave resonance frequency of about 9.1 GHz.

X-ray diffraction (XRD) spectra were recorded on a Philips PW 1820 spectrometer between 2° and 90° (2θ), with 0.05° increment and acquisition time of 20 s.

The oxidation behavior was followed using a B60 Setaram thermobalance coupled to a quadrupole mass spectrometer (MS. Quadrex 200, 70 eV, electron impact). The powder was heated under a mixture of gas (2% O₂ in He). The oxygen consumption and the release of gases were simultaneously analyzed.

Results

Characterization of the Oxycarbide Phase. The characterization of the oxycarbide phase obtained after pyrolysis at 1000 °C, has already been reported³³ and will only be summarized in this paper. The X-ray diffraction pattern is characteristic of an amorphous material and the main structural characterization came from MAS NMR experiments. The ²⁹Si NMR spectra have clearly shown the existence of Si-C bonds in the pyrolyzed samples through the presence of resonances at -72 ppm (35%) due to SiCO_3 sites, at -32 ppm (8%) due to SiC_2O_2 sites and at -8 ppm (2%) due to SiC_3O sites. The major component is due to SiO_4 sites (55%).²⁶ Recently, Mutin et al. have shown that the environment of silicon atoms in the oxycarbide phase depends only on the O/Si ratio in the glass, and not on the structure of the precursors:³⁵ it corresponds to a purely random distribution of Si-O and Si-C bonds. For O/Si = 1.7, the calculated percentages of the various Si sites are the followings: 52.20% of SiO_4 , 36.85% of SiCO_3 , 9.75% of SiC_2O_2 , 1.15% of SiC_3O , and 0.05% of SiC_4 . The results obtained on the present oxycarbide glass with O/Si = 1.64 are in good agreement with these calculations, showing that the oxycarbide network can be described with randomly distributed $\text{SiC}_x\text{O}_{4-x}$ units. This oxycarbide glass derived from a starting gel with SiC_2O_2 and SiO_4 units, is close to that obtained by Mutin from a gel prepared from methyltrimethoxysilane, and thus containing only SiCO_3 units. Both gels have in fact, very similar O/Si ratios, 1.64 and 1.69.

A comparison between chemical analysis ($\text{SiC}_{0.58}\text{O}_{1.64}$) and NMR results obtained on the oxycarbide phase suggested that ≈ 75 mol % of the carbon (≈ 8 wt %) is present in a free carbon phase. Indeed, formation of aromatic carbon was clearly evidenced by ¹³C CP MAS NMR. The sample pyrolyzed at 1000 °C for 1 h still

(34) Massiot, D.; Thiele, H.; Germanus, A. *Bruker Rep.* **1994**, *140*, 43.

(35) Corriu, R. J. P.; Leclercq, D.; Mutin, P. H.; Vioux, A. *Mater. Res. Soc. Symp. Proc.* **1994**, *346*, 351.

Table 1. Elemental Analysis on Pyrolyzed Samples, Ceramic Yields (Y), and Silicon and Carbon Losses (ΔSi and ΔC)

temp (°C)	chemical analysis ^a				char yield (wt %)	ΔSi (%)	ΔC (%)
	%Si	%C	%O ^b	emp formula			
1000 (5 °C/min; 10 min)	46.5	11.2	41.2	SiC _{0.56} O _{1.55}	78	14	48
1200 (5 °C/min; 10 min)	45.2	10.4	44.4	SiC _{0.53} O _{1.72}	74	16	54
1400 (10 °C/min; 10 min)	48.6	10.6	40.8	SiC _{0.51} O _{1.47}	71	18	56
1500 (10 °C/min; 1 h)	50.0	10.8	39.2	SiC _{0.50} O _{1.37}	63	21	60
1500 (10 °C/min; 1 h)	45.5	9.9	44.5	SiC _{0.51} O _{1.71}	45	49	74
1500 (10 °C/min; 10 h)	46.8	9.4	43.8	SiC _{0.47} O _{1.64}	34	47	81
1500 (2 °C/min; 10 min)	46.1	10.1	43.7	SiC _{0.51} O _{1.66}	71	19	58
1500 (5 °C/min; 1 h)	44.5	10.5	45.0	SiC _{0.55} O _{1.77}	70	23	57
1500 (25 °C/min; 10 min)	45.7	11.2	43.1	SiC _{0.57} O _{1.65}	72	19	52
1600 (10 °C/min; 10 min)	45.5	10.6	43.9	SiC _{0.54} O _{1.69}			

^a Hydrogen was always less than 0.2 wt % except in the 1000 °C sample, 1.0 wt %. ^b Oxygen was estimated by difference.

exhibits a high surface area ($\approx 100 \text{ m}^2/\text{g}$), and this was related to the presence of adsorbed water in the sample, as detected by infrared analysis.

Thermal Evolution of the Oxycarbide Samples under Argon. The oxycarbide sample was fired under flowing argon to various temperatures. Experimental conditions are presented in Table 1. The char yield is almost constant from 1000 to 1400 °C, $75 \pm 5 \text{ wt } \%$. At 1500 °C, the char yield decreases strongly with holding time to reach 34 wt % after 10 h. Elemental analysis have been performed on the fired samples (Table 1). The losses of silicon and carbon were estimated using the formula introduced by Mutin et al.:¹⁶

$$\Delta X = 100((\%X)_0 - Y(\%X)_T)/(\%X)_0 \quad (1)$$

where $(\%X)_0$ and $(\%X)_T$ are the mass percentages of the X element in the gel precursor and in the pyrolyzed sample and Y is the char yield. All the results are reported in Figure 1. The large weight losses observed at 1500 °C are related with losses of carbon and especially silicon, most likely in the form of gaseous CO and SiO.

Structural evolution of the pyrolyzed samples has been investigated using ²⁹Si MAS NMR spectroscopy. The spectra were simulated and the results are presented in Figure 2. Five possible components were used at $-110 \pm 2 \text{ ppm}$ (SiO_4), $-74 \pm 3 \text{ ppm}$ (SiCO_3), $-36 \pm 3 \text{ ppm}$ (SiC_2O_2), $-4 \pm 2 \text{ ppm}$ (SiC_3O), and $-13 \pm 5 \text{ ppm}$ (SiC_4) and the percentages of the various Si sites extracted. Due to the rather low signal/noise ratios, these quantitative data can not be of high accuracy. In addition, the assignment of the broad overlapped signals which range between 0 and -40 ppm is rather delicate. Thus these results are presented to give a general trend in the evolution of the various $\text{SiC}_x\text{O}_{4-x}$ sites. All the various components show the same trend: they shift upfield continuously with the firing temperature.

The quantitative evolution of the various Si units is presented in Figure 3: the number of mixed $\text{SiC}_x\text{O}_{4-x}$ units ($x = 1, 2, 3$) decreases with pyrolysis temperature while the number of SiC_4 and SiO_4 units increases, indicating that a phase separation occurs between a silica-rich phase and a silicon carbide-rich phase.

The number of Si-C bonds per Si site was calculated by the following relation:

$$n_{\text{Si-C}} = (4 \cdot \% \text{SiC}_4 + 3 \cdot \% \text{SiC}_3\text{O} + 2 \cdot \% \text{SiC}_2\text{O}_2 + \% \text{SiCO}_3)/100 \quad (2)$$

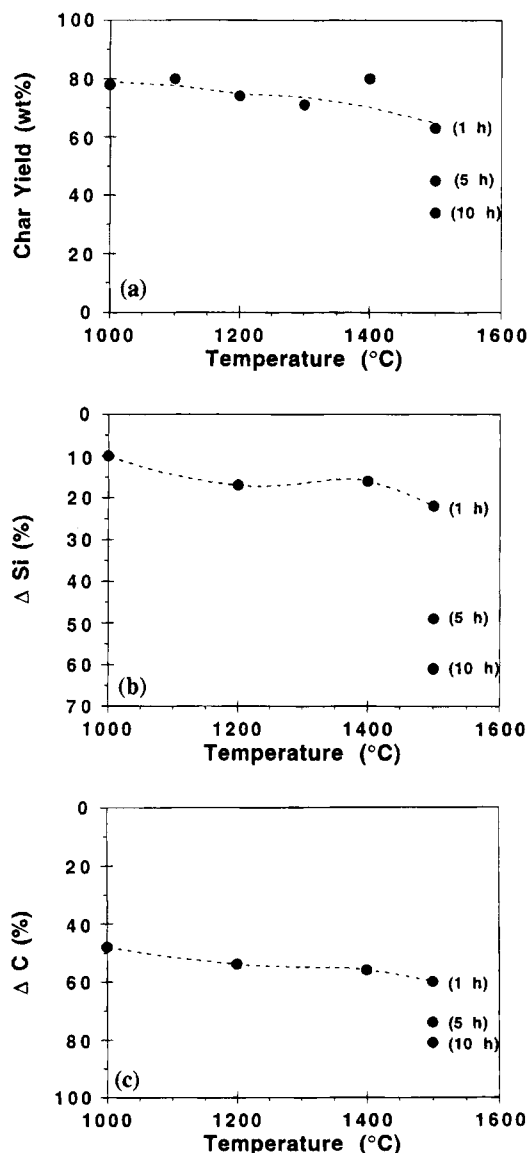


Figure 1. : Evolution of char yields (a) and losses of silicon (b) and carbon (c) versus pyrolysis temperatures. Heating rate 10 °C/min; holding time 10 min except at 1500 °C, 1 h, 5 h, and 10 h.

It is almost constant up to 1300 °C, $n_{\text{Si-C}} \approx 0.6$ (Figure 4). Then above 1300 °C, the number of Si-C bonds increases ($n_{\text{Si-C}} \approx 0.9$ at 1500 °C), and this is favored by longer holding times. After 10 h at 1500 °C, $n_{\text{Si-C}} \approx 1.0$.

Assuming that the C atoms present in the silicon oxycarbide phase are bonded to four silicon atoms, it is possible to estimate from the ²⁹Si NMR simulations, the

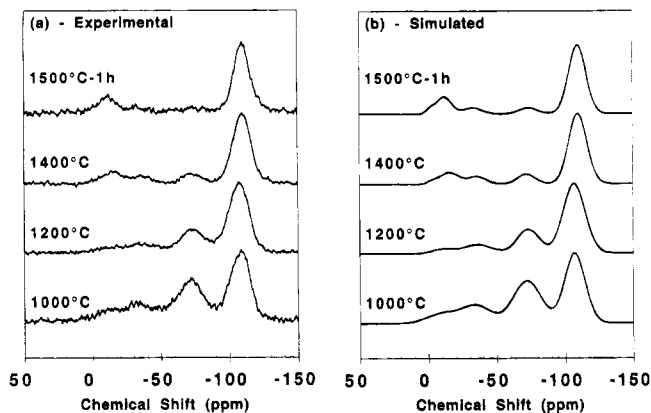


Figure 2. Experimental (a) and simulated (b) ^{29}Si MAS-NMR spectra of pyrolyzed samples. Heating rate $10^\circ\text{C}/\text{min}$; holding time 10 min except at 1500°C , 1 h.

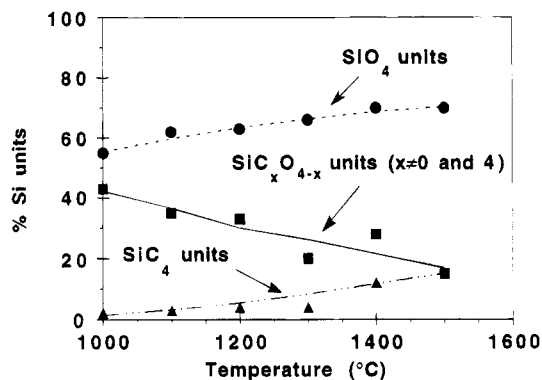


Figure 3. Evolution of the number of Si sites versus pyrolysis temperature. Heating rate $10^\circ\text{C}/\text{min}$; holding time 10 min except at 1500°C , 1 h.

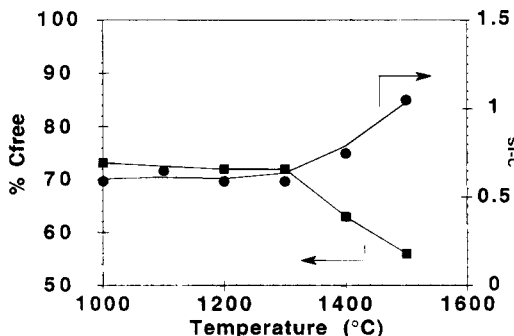


Figure 4. Evolution of the average number of Si-C bonds per Si sites units and of the free carbon content in the pyrolyzed samples. Heating rate $10^\circ\text{C}/\text{min}$; holding time 10 min except at 1500°C , 1 h.

number of carbon per silicon in this phase:

$$nC_{\text{oxy}} = (\% \text{SiC}_4 + 0.75 \cdot \% \text{SiC}_3\text{O} + 0.5 \cdot \% \text{SiC}_2\text{O}_2 + 0.25 \cdot \% \text{SiCO}_3) / 100 \quad (3)$$

A comparison with elemental analysis which gives the total amount of carbon, nC_{tot} , allows to estimate the percentage of C present in the free carbon phase:

$$\%C_{\text{free}} = (nC_{\text{tot}} - nC_{\text{oxy}}) / nC_{\text{tot}} \quad (4)$$

The evolution of $\%C_{\text{free}}$ versus temperature (Figure 4) seems closely related with the evolution of the average number of Si-C bonds per silicon: the percentage of free carbon is constant up to 1300°C (≈ 75 mol %) and then decreases to 55 mol % in the 1500°C sample pyrolyzed for one hour.

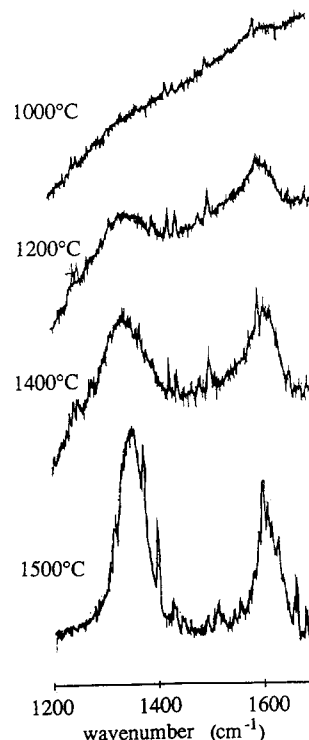


Figure 5. Raman spectra of the pyrolyzed samples. Heating rate $10^\circ\text{C}/\text{min}$; holding time 10 min except at 1500°C , 1 h.

^{13}C MAS NMR experiments could not be performed easily on pyrolyzed samples, because of long ^{13}C relaxation times in these systems and presence of a probe signal in the region due to aromatic C atoms. Cross-polarization techniques which were of great utility for samples pyrolyzed at low temperatures³³ ($T < 1000^\circ\text{C}$) cannot be applied for these samples because of the large decrease in hydrogen content. Raman experiments were carried out to get information on the structural evolution of the carbon phase. The spectra of the samples pyrolyzed between 1200 and 1500°C are shown in Figure 5.

The Raman spectrum of the 1000°C sample consists of a very broad fluorescence signal. This signal which almost disappears for samples pyrolyzed between 1400 and 1500°C , could come from radical species which have been evidenced by ESR.³³ In the 1000°C sample, the concentration of radical species was estimated to $\approx 3.0 \times 10^{19}$ spins/g, while at 1500°C , this value decreases to $\approx 2.5 \times 10^{18}$ spins/g. Despite this fluorescence signal, the Raman spectrum of the 1000°C sample shows two hardly visible Raman bands at ≈ 1300 and $\approx 1600\text{ cm}^{-1}$. In the spectrum of the 1200°C sample, these two signals at 1360 and 1620 cm^{-1} become more intense. For the 1500°C sample, the intensity of the 1360 cm^{-1} signal is higher than that at 1620 cm^{-1} , and the signals are strongly sharpened.

These two bands are characteristic of disordered graphitic forms of carbon.^{37,38} The Raman spectrum of graphite presents one band at 1590 cm^{-1} (E_{2g} mode). The 1600 cm^{-1} vibration is thus usually referred as the G band. The 1360 cm^{-1} is commonly called D band, for defect band. It corresponds to the A_{1g} mode of graphite, which is theoretically Raman inactive in perfect graph-

(37) Wang, Y.; Alsmeyer, D. C.; McCreery, R. L. *Chem. Mater.* **1990**, *2*, 557.

(38) Knight, D.; White, W. B. *J. Mater. Res.* **1989**, *4*, 385.

Table 2. Results of the Simulations of the ^{29}Si MAS NMR Spectra

sample	chemical shift in ppm (% Si units)				
	SiO_4	SiCO_3	SiC_2O_2	SiC_3O	SiC_4
1000 °C	-109 (55)	-71 (35)	-33 (8)		-8 (2)
1100 °C	-111 (62)	-72 (19)	-33 (15)		-11 (4)
1200 °C	-118 (63)	-72 (22)	-35 (11)		-9 (4)
1300 °C	-110 (66)	-70 (18)	-37 (11)		-15 (5)
1400 °C	-110 (70)	-72 (9)	-36 (7)	-3 (1)	-16 (12)
1500 °C	-111 (70)	-76 (6)	-35 (6)	-3 (2)	-14 (16)
1500 °C (1 h)	-110 (65)	-76 (2)	-34 (13)	-6 (3)	-18 (17)
1500 °C (10 h)	-111 (68)		-38 (12)		-18 (20)

Table 3. Evolution of the Relative Intensity (I_D/I_G), Peak Frequency (w), and Full Width at Half-Maximum (fwhm) of the D and G Bands of the Raman Spectra with the Pyrolysis Temperature

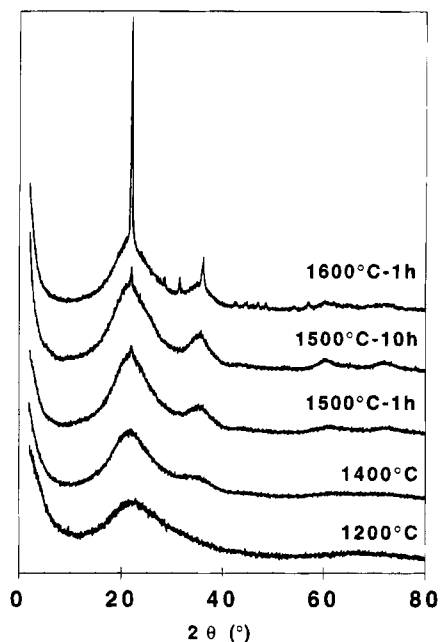
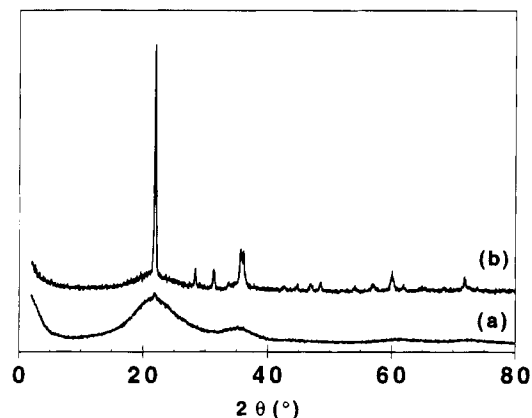
pyrolysis parameters	I_D/I_G	w_D (cm^{-1})	fwhm $_D$ (cm^{-1})	w_G (cm^{-1})	fwhm $_G$ (cm^{-1})
1200 °C	1.3	1340	150	1600	80
1400 °C	1.4	1346	100	1605	64
1500 °C; 1 h	1.9	1357	54	1610	58
1500 °C; 10 h	2.2	1362	52	1600	75

ite crystals. However, this band appears in every polycrystalline graphitic material, pyrolytic carbon or vitreous carbon.³⁹ The intensity ratio between the D and G bands (I_D/I_G) can provide indication about the graphitic domain sizes,^{36,38,39} while the line width of the G band can be related to disorder between the carbon sheets.³⁹ The spectral parameters of these two bands for the various pyrolyzed samples are reported in Table 3: the position of the two bands shift slightly toward higher wavenumbers, especially the position of the D band, while they simultaneously sharpen. The intensity ratio I_D/I_G increases with firing temperature from 1.3 at 1200 °C to 1.9 at 1500 °C. These values indicate that the particle size is quite small around 3–4 nm.³⁸ The band shape parameters of the 1200 and 1400 °C samples are close to those of coke, corresponding to highly disordered carbons, while the parameters of the 1500 °C correspond more to glassy carbon.³⁸

X-ray diffraction patterns are presented in Figure 6. For the 1200 °C sample, the pattern consists of a broad signal centered at $2\theta = 21^\circ$, characteristic of amorphous silica.⁴⁰ For the 1400 °C sample, it shows new broad peaks at $2\theta \approx 35^\circ$, 60° , and 70° due to the crystallization of $\beta\text{-SiC}$.⁴¹ These signals sharpen with the pyrolysis temperature, but still remain broad after 1 h at 1500 °C or at 1600 °C. Above 1500 °C, formation of crystalline SiO_2 cristobalite⁴² is detected through the presence of sharp signals at $2\theta = 22.0^\circ$, 28.5° , 31.5° , and 36.1° . This crystalline phase is even more present in the sample fired at 1500 °C for 10 h.

TEM experiments performed on the 1500 °C sample fired for 1 h show a very featureless microstructure, characteristic of a poorly ordered material. Some diffraction rings due to the presence of $\beta\text{-SiC}$ crystallites were observed.

A silica gel mixed with amorphous carbon was prepared with a C/Si ratio similar to that of the starting

**Figure 6.** XRD patterns of the pyrolyzed samples. Heating rate 10 °C/min.**Figure 7.** XRD patterns of (a) the silicon oxycarbide sample and (b) a mixture of silica and carbon pyrolyzed under the same conditions. Heating rate 10 °C/min; maximum temperature 1500 °C; holding time 1 h.

gel from DMDES and TEOS, i.e., C/Si = 1. This sample was pyrolyzed at 1000 and 1500 °C in order to compare the crystallization behavior of the two systems. The 1000 °C sample (C/Si = 0.86), is amorphous while the XRD pattern of the 1500 °C sample (C/Si = 0.4) shows sharp diffraction peaks due to the formation of cristobalite SiO_2 and silicon carbide $\beta\text{-SiC}$ (Figure 7).

Oxidation Behavior of Oxycarbide Samples. The oxidation behavior of oxycarbide samples has been examined using TG/MS analysis. The TG curves were recorded under flowing pure oxygen. The TG curve of the 1200 °C sample (Figure 8) shows a first weight gain of 0.2% between 500 and 800 °C and then a continuous weight gain with an increasing oxidation rate above 1000 °C. The total weight gain is 1% at 1400 °C. For the 1500 °C sample, the weight gain starts only at 900 °C, but the total weight gain is still 1%.

To better define the oxidation of the various phases present in the materials, evolved gas analysis by mass spectrometry has been used. This technique follows the oxygen uptake from a mixed gas (2% O_2 /helium) by the pyrolyzed sample, as well as the gases released during

(39) Lespade, P.; Marchand, A.; Couzi, M.; Cruege, F. *Carbon* **1984**, *22*, 375.

(40) Warren, R. E. *J. Am. Ceram. Soc.* **1934**, *17*, 24.

(41) JCPDS File 29 1129.

(42) JCPDS File 11 695.

(43) Bahloul, D.; Pereira, M.; Goursat, P. *Ceram. Int.* **1992**, *18*, 1.

(44) Biernacki, J. J.; Wotzak, G. P. *J. Am. Ceram. Soc.* **1989**, *72*, 122.

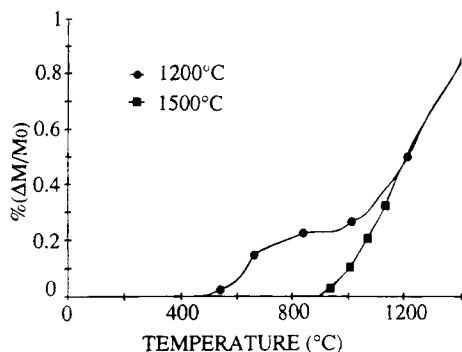


Figure 8. TG curves under O_2 of the samples pyrolyzed at 1200 and 1500 °C.

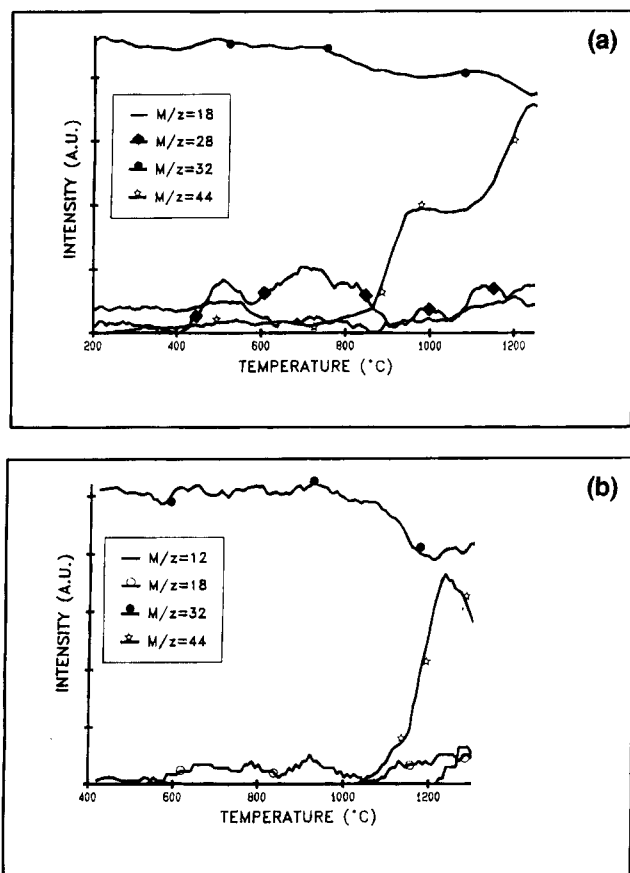
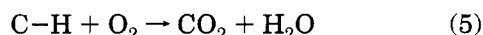


Figure 9. MS analysis of the gas evolution during the heat treatment of the pyrolyzed samples under a mixture of He/2% O_2 : (a) 1200 °C and (b) 1500 °C pyrolyzed samples.

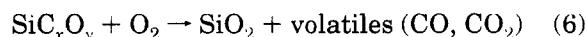
the reaction. MS curves are shown in Figure 9 for the 1200 and 1500 °C (1 h) samples.

The oxidation of the 1200 °C sample leads to a departure of CO_2 ($m/z = 44$) and H_2O ($m/z = 18$) in the 400–800 °C temperature range which coincides with the slight intake of oxygen ($m/z = 32$). The peak due to $m/z = 44$ could also correspond to SiO , but the presence of the $m/z = 12$ fragment due to C^{2+} confirms its attribution to CO_2 . In this temperature range, it has often been reported that the departure of these gases (CO_2 , H_2O) correspond to the combustion of free carbon by the following reaction:



However, this reaction is characterized by a weight loss and thus is not consistent with the weight gain observed by TGA (Figure 8). This weight gain seems

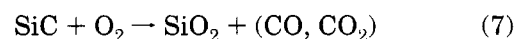
more related with the oxidation of the silicon oxycarbide phase:



Thus, it can be noted that the carbon, present in the 1200 °C product, appears to be embedded in a continuous silicon oxycarbide phase and is not easily oxidized.

Both reactions 5 and 6 could occur simultaneously and this could explain the changes in the oxidation rate observed by TGA (Figure 8).

Above 800 °C, an important loss of CO_2 ($m/z = 44$) is observed which occurs in two steps. This suggests the existence of at least two different species in the solid product. According to the weight gains observed in the TG curve (Figure 8), the peaks at $m/z = 44$ (CO_2) can be interpreted as the oxidation of silicon oxycarbide phases having different compositions, and also by the oxidation of silicon carbide, according to reactions 6 and 7:



For the 1500 °C sample, the TG curve exhibits a rapid increase in the weight gain above 900 °C due to the formation of silica. The MS profile of the $m/z = 44$ peak is similar to the behavior found for the 1200 °C sample, above 1100 °C. This could essentially correspond to the oxidation of the silicon carbide phase, which was detected by X-ray diffraction and ^{29}Si NMR.

Whatever the pyrolysis temperature is, 1200 or 1500 °C, these materials thus show a good oxidation resistance, at least in the short term, despite the presence of carbon-containing phases. However, their oxidation behavior is different, certainly because of different microstructures.

The difference in temperature observed between the TGA and MS can be explained by the difference of oxygen pressure used during the two types of analyses.

Discussion

The high-temperature behavior of the oxycarbide samples under argon, can be divided in three main steps:

(1) **From 1000 to 1300 °C.** The samples are obtained with an almost constant char yield, ≈ 75 wt %. They are X-ray amorphous, but the ^{29}Si MAS NMR shows clearly the presence of a distribution of SiC_xO_{4-x} sites, with SiO_4 as the major component. In this temperature range, the average number of Si–C bonds per Si site does not vary (Figure 4), but the distribution of SiC_xO_{4-x} sites does change (Figure 3): this is clearly due to redistribution reactions between Si–C and Si–O bonds leading to domains rich in Si–O bonds and domains rich in Si–C bonds according to:



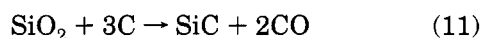
Such reactions have already been mentioned in the literature in the same temperature range for siloxane-derived oxycarbide samples.¹⁴

The free carbon phase, which formed during the polymer-to-ceramic conversion around ≈ 700 °C,³³ is still

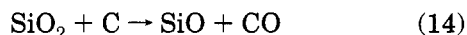
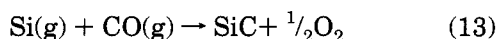
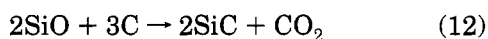
present as revealed from a comparison between the NMR data and the chemical analysis. Its percentage does not change over this temperature range and represents ≈ 75 mol % of the total carbon. Some information on the structure of this phase can be extracted from the Raman bands whose spectral parameters are characteristic of highly disordered carbons such as charcoal or coke.³⁸ The results of the TG and MS analyses during oxidation (Figures 8 and 9) suggest that the free carbon is embedded in a continuous glassy silicon oxycarbide phase and thus is not readily exposed to oxidation.

(2) From 1300 to 1500 °C. The char yield is still stable around 75 wt %, showing no major gas losses. However, the chemical composition of the oxycarbide phase changes, according to the ²⁹Si MAS NMR spectra, with an increase in the number of Si-C bonds (Figure 4). This is in agreement with the X-ray diffraction pattern of the 1400 °C sample which reveals the presence of small β -SiC crystallites. Simultaneously, the free carbon content seems to decrease. The Raman spectra show an ordering of the carbon phase, with particle size around 3–4 nm. Siloxane derived oxycarbide phases, compositionally stable up to ≈ 1500 °C, have already been reported in the literature.^{14,45} This is a surprising result, considering the observed high temperature behavior of the Nicalon fibers: evidence for a silicon oxycarbide phase was found in these fibers,⁴⁶ which is responsible for their degradation at $T > 1200$ °C, caused by carbothermal reactions with free carbon.^{47,48} This point should be further investigated.

(3) At 1500 °C. At this temperature, the char yield decreases dramatically with holding time, strongly suggesting that at this temperature, carbothermal reactions occur in the system. The Si-C-O system is known to be unstable in this temperature range.^{47–49} Carbothermal reaction between silica and carbon to produce SiC is well-known:



Other reactions should be also considered:^{44,50}



The latter is in perfect agreement with the loss of silicon observed with long holding times (Figure 1).

(45) Sorarù, G. D.; D'Andrea, G.; Camprostrini, R.; Babonneau, F.; Mariotto, G.; *J. Am. Ceram. Soc.*, in press.

(46) Porte, L.; Sartre, A. *J. Mater. Sci.* **1989**, *24*, 271.

(47) Mah, T.; Hecht, N. L.; McCullum, D. E.; Hoenigman, J. R.; Kim, H. M.; Katz, A. P.; Lipsitt, H. A. *J. Mater. Sci.* **1984**, *19*, 1191.

(48) Jonhson, S. M.; Brittain, R. D.; Lamoreaux, R. H.; Rowcliffe, D. R. *J. Am. Ceram. Soc.* **1988**, *71*, C132.

(49) Luthra, K. L. *J. Am. Ceram. Soc.* **1986**, *69*, C 231.

(50) Klinger, N.; Strauss, E. L.; Komarek, K. L. *J. Am. Ceram. Soc.* **1966**, *49*, 369.

Formation of silicon carbide is clearly observed by X-ray diffraction and ²⁹Si MAS NMR. However, the crystallite size remains very small, ≈ 2 –3 nm, even after 10 h at 1500 °C. At this temperature, the mixed $\text{SiC}_x\text{O}_{4-x}$ units ($x \neq 0$ and 4) have almost all disappeared and the system can be described as a matrix of poorly crystalline silica in which small silicon carbide particles are dispersed. A free carbon phase is still present as evidenced by the Raman spectra. The spectral parameters, compared to those found for the 1200 °C sample correspond to more ordered carbon phases such as glassy carbon. However, the intensity ratio (I_D/I_G) is quite high, suggesting very small carbon particles. The comparison of the crystallization behavior of this system with that of a mixture of silica gel and carbon clearly shows a high resistance to crystallization of these oxycarbide samples.

These samples are also resistant to oxidation: in the 1500 °C sample, the oxidation starts only above 1000 °C, compared to 400 °C in the 1200 °C sample. This can be related to the presence of less free carbon which has been consumed according to reaction 11, as well as less mixed $\text{SiC}_x\text{O}_{4-x}$ sites ($x \neq 4$) which seem much more reactive to oxidation than SiC.

Conclusion

The high temperature behavior of silicon oxycarbide samples obtained through the pyrolysis under inert atmosphere of methyl-containing silica gels was investigated, using elemental analysis, ²⁹Si MAS NMR spectroscopy, Raman spectroscopy, and X-ray diffraction. The starting sample, pyrolyzed at 1000 °C, can be described as a main oxycarbide phase with a random distribution of $\text{SiC}_x\text{O}_{4-x}$ units and an additional free carbon phase. Up to 1300 °C, the system undergoes redistribution reactions between Si-C and Si-O bonds leading to a phase separation between domains rich in SiC_4 units and others rich in SiO_4 units. Between 1300 and 1500 °C, the system is still compositionally stable. The NMR data seems to indicate an enrichment in Si-C bonds of the oxycarbide phase, which is related to a decrease in the free carbon content. However, no important weight loss are observed. At 1400 °C, small SiC crystallites start to form. It is only at 1500 °C with increasing holding times that the char yields strongly decrease, indicating carbothermal reduction reactions between the oxycarbide and the free carbon phases. However, the samples remain poorly crystalline, showing a high resistance to crystallization. Their good oxidation resistance is also a positive point for these systems, if applications in the field of high-temperature materials are considered.

Acknowledgment. The authors would like to greatly acknowledge Dr. Elisabeth Tronc for helpful discussions on XRD experimentation, Dr. Geneviève Chottard for the Raman experiments, and Mr. Lavergne for TEM experiments.

CM9405638